BASIS OF ELECTROMAGNETIC COMPATIBILITY OF INTEGRATED CIRCUIT

Chapter V - MODELLING PASSIVE DEVICES

Corrections of exercises

I. EXERCISE NO 1 - Modelling passive devices

The impedance profile of four passive devices has been measured with a VNA. The component references, the measured impedance profiles and the measurement result files are shown below. The measurement files can be found in directory book/ch5. With IC-EMC, build an electrical model for the four devices. The references of the measured devices are given. You can refer to their specifications to build the model.

Ceramic capacitor	Iron powder inductor
Kemet C0805C103K5RACAUTO	Vishay IHLP4040DZER470M11
(Ceramic_capacitor.s1p)	(Iron_Powder_inductor.s1p)
Electrolytic aluminium capacitor	Chip ferrite bead
Panasonic EEEFP1C470AP	Murata BLM21PG600SN1D
(Aluminum_capacitor.s1p)	(Ferrite_bead.s1p)
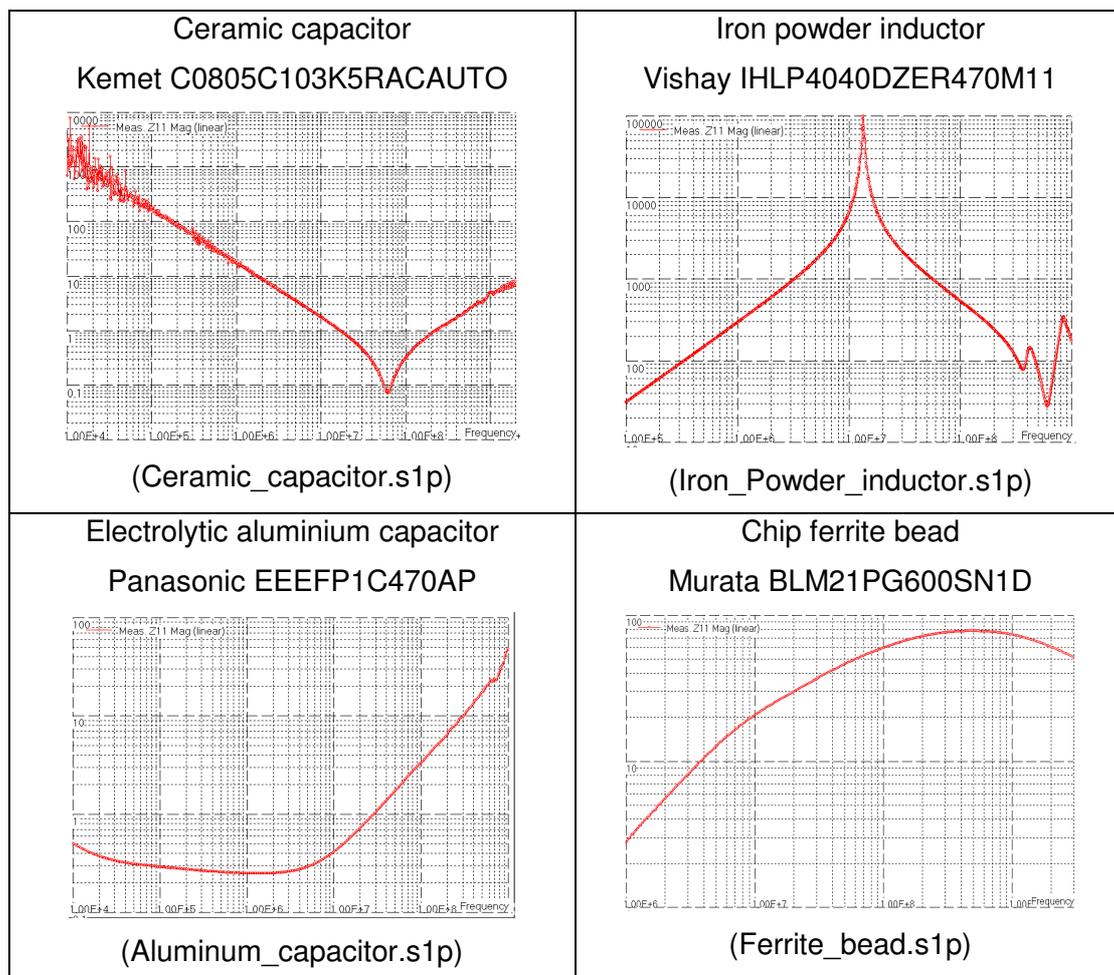
Corrections:

Modeling of ceramic capacitor: with the reference number of the device and the datasheet, the capacitance value can be deduced: 10 nF. A fit of the capacitance value from the measurement provides a more precise value: 9.3 nF. The measurement shows a LC resonant frequency at 62 MHz. The equivalent electrical model is a serial L-C circuit, where the inductance is about 0.73 nH. Effects of losses are mostly visible near the resonances. They are modeled by a single and constant resistance equal to 66 mΩ. The equivalent model and a comparison between measured and simulated impedances are shown below.

.AC DEC 100 1k 1G

Electrical model of a 10 nF Aluminum capacitor (Kemet C0805C103K5RACAUTO)
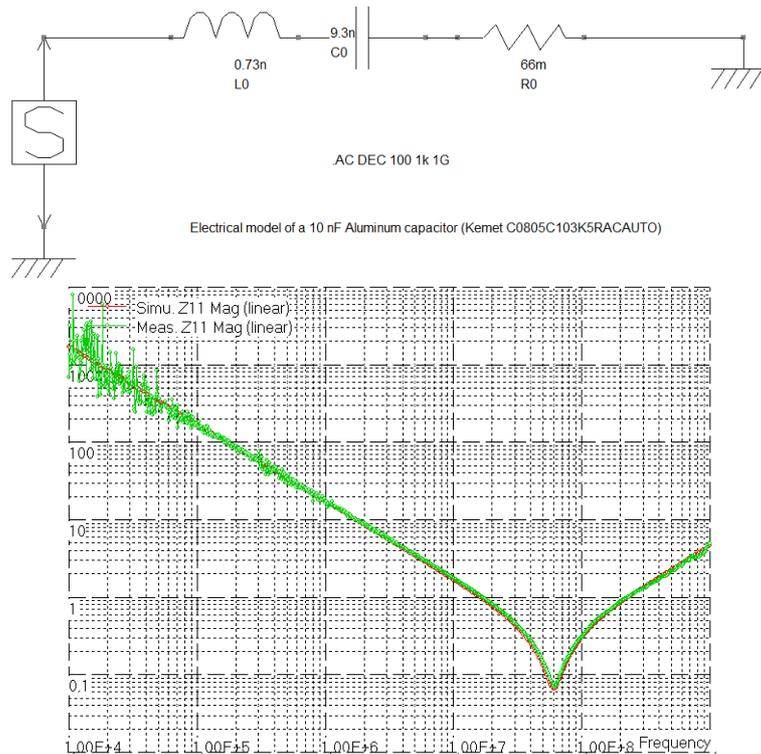
Modeling of electrolytic aluminum capacitor: with the reference number of the device and the datasheet, the nominal capacitance value can be deduced: 47 µF.However, the variability on this type of capacitor is important (the tolerance on the capacitance is 20 %), so the exact capacitance value is adjusted from the measured impedance curve (39 µF). The effect of the parasitic inductance is visible above 10 MHz. The inductance value L0 is extracted from the measured impedance above 10 MHz: 5.4 nH. A clear L-C resonance is not visible due to the high losses of this type of capacitor. Moreover, the losses are frequency dependent and tend to decrease with frequency. In order to model this trend, the methodology presented in part 5.4.b is used.The frequency dependence of the ESR is modeled by a constant resistance R_0 followed by a serie of N parallel RC branches. The sum of all the resistances is equal to the resistance at the start frequency of the frequency range where the ESR dominates. The poles of each RC branches are ditributed over this frequency range.

In the model proposed below, the number of parallel RC branches N = 2. This simple solution gives an acceptable result, but N can be increased to improve the accuracy of the model. The start frequency is chosen at 40 kHz, where the resistance is about 0.32 Ω. The ESR decreases between 40 kHz and 1 MHz. The two poles of the R_1-C_1 and R_2-C_2 branches are placed within this range, at nearly 100 and 340 kHz.Given the previous conditions and the resistances at 100 kHz and 340 kHz, the values of R_0, R_1, R_2, C_1 and C_2 are selected and adjusted to improve the fit between measured and simulated impedances. Real and imaginary parts of the impedance can laso be dislayed to evaluate the fit between measurement and simulation.

Electricla model of a 47 µF Aluminum capacitor (Panasonic EEEFP1C470AP)
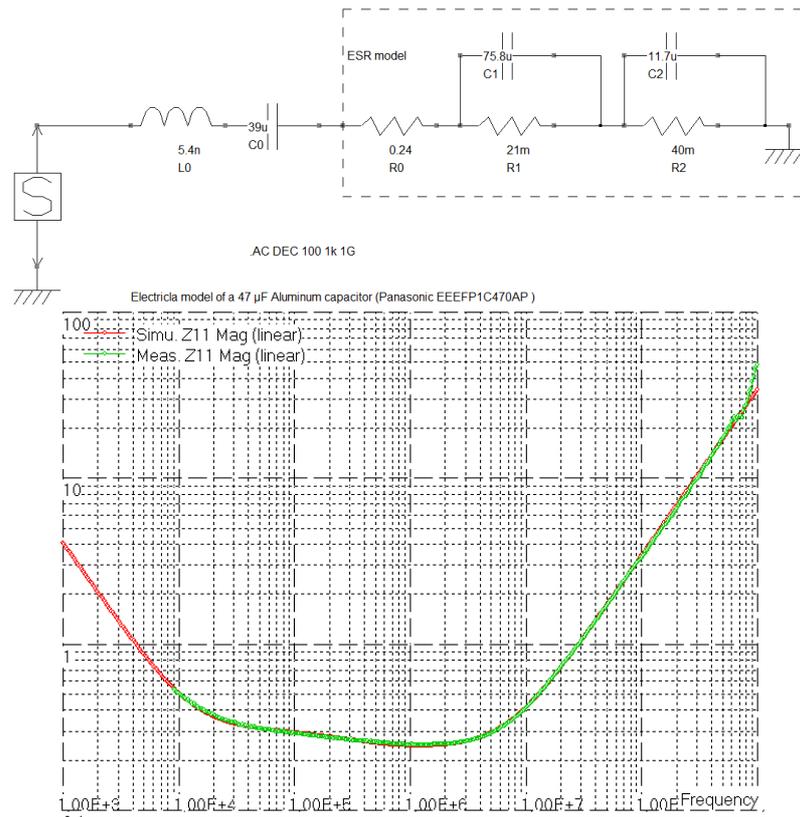
Modeling of iron powder inductor: with the reference number of the device and the datasheet, the nominal inductance L_0 and the DC resistance R_S values are deduced: 47 µH and 130 mΩ. A generic model for an inductance is proposed, as the one shown in Fig. 5-24. The inductance is verified by the measured impedance below 1 MHz where the imductive behavior dominates. The measurement shows a resonant frequency at 13.4 MHz, which is modeled by a parallel L-C. The parasitic capacitance is 3 pF. A parallel resistance Rp is also added to take into account the core losses. In this model, the losses are supposed constant, so resistance values R_S and Rp are also constant. Rp value is adjusted to fit the impedance around the resonance frequency. The model is described below, and the comparison between measured and simulated impedance is presented below. A good fit is ensured up to 200 MHz. Above this frequency, numerous resonances appear due to the relatively large physical size of the inductor. The inductance, parasitic capacitance and loss resistance should be distributed in several RLC cell to improve the fit, as described in Fig. 5-26 and 5-27.

Electricla model of a 47 µH iron powder inductor (Vishay IHLP4040DZER470M11)
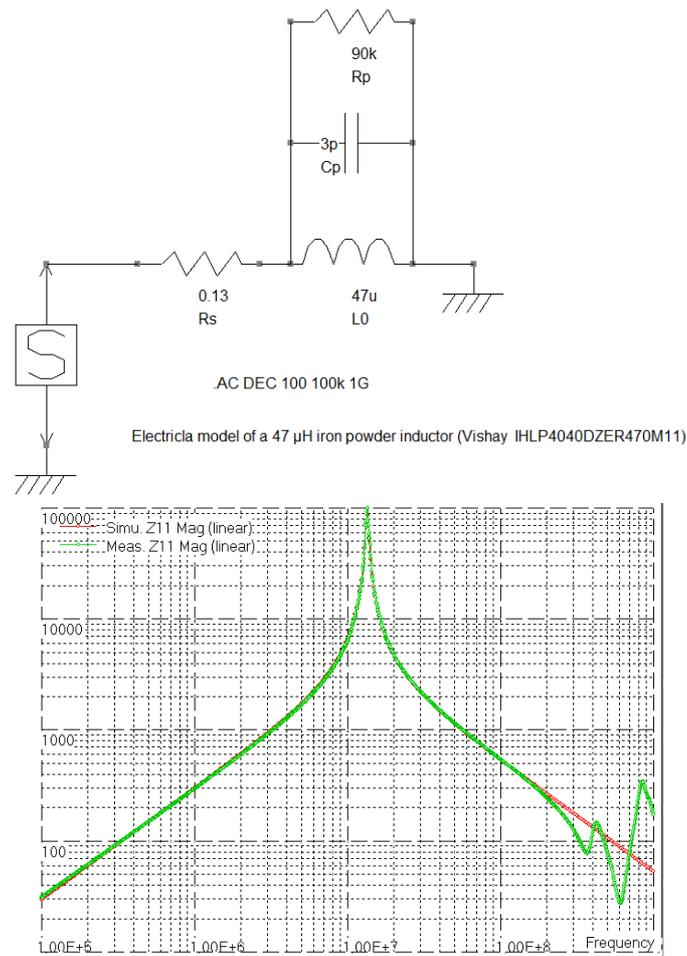
Modeling of ferrite bead: Modeling a ferrite bead is quite complex since it is a lossy magnetic material: both the inductance and the loss resistance are frequency dependent.The datasheet specifies only the DC resistance (the resistance Rdc of the model equal to 20 mΩ) and the impedance at 100 MHz, but this parameter is not sufficient to build an equivalent model.The methodology to build the equivalent model is explained in part 6.3. The device is very close to the ferrite bead presented in part 6.3.

The equivalent model consists in a serie of N parallel Li-Ri cells that ensures a nearly constant imaginary part of the impedance and an increase of its real part over a given frequency range.The cut-off frequencies of the N cells over this frequency range.

In the proposed model, we use 3 L-R cells. More cells can be used to improve the model.The inductive behaviour dominates up to 5 MHz and the total inductance is about 440 nH. From the measurement, the sum of the three inductance must be equal to this inductance. The imaginary part increases slowly and starts decreasing between 8 and 200 MHz, while the real part increases strongly. The three cut-off frequencies of the L-R cells are spread over the frequency range 8 - 200 MHz. The imaginary part of the imepdance become negative and its real part decrease above 500 MHz. This effect is due to a parallel capacitance. However, it is difficult to set the exact value of the capacitance: no L-C resonance arises due to the high losses of this component. The value of the capacitance Cp is adjusted to fit the simulated impedance on the measurement. Cp short-circuit only the two first cells,to limit the impedance decrease above 500 MHz.

The following figures present the equivalent model and the comparison between measured and simulated impedance.

310n
L1

100n
L2

34n
L3

0.02
Rdc

18
R1

30
R2

35
R3

1.8p
C1
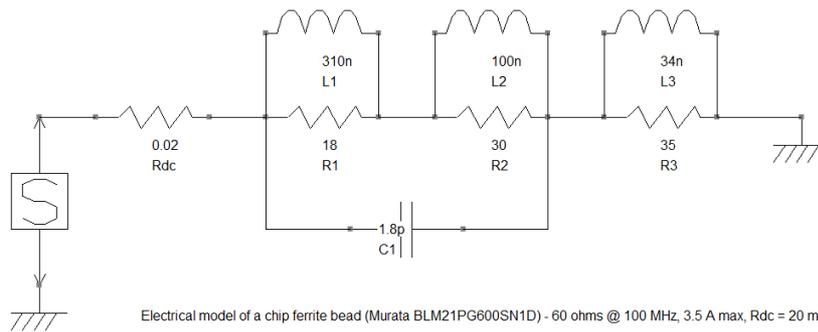
Electrical model of a chip ferrite bead (Murata BLM21PG600SN1D) - 60 ohms @ 100 MHz, 3.5 A max, Rdc = 20 mohms

.AC DEC 100 1MEG 3G

100
Simu. Z11 Mag (linear)
Meas. Z11 Mag (linear)

10

1.00E+6   1.00E+7   1.00E+8   1.00E Frequency
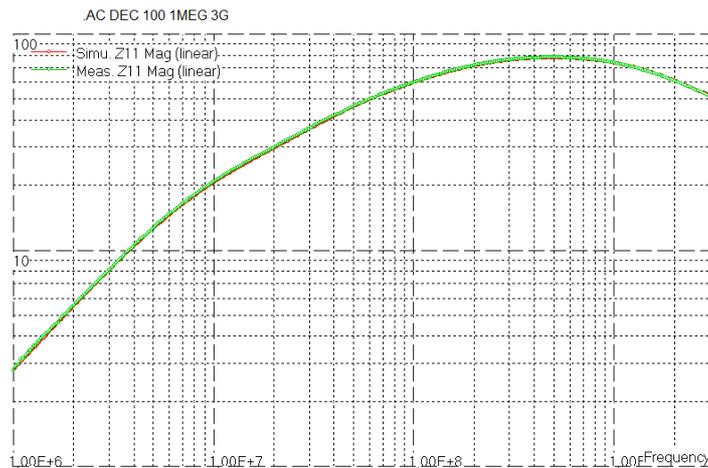
II. EXERCISE NO 2 - EMI filter for an AC line

The following diagram shows the general structure of an EMI filter for an AC power supply line. It is dedicated to the suppression of common- and differential-mode noise coupled on phase (L) and neutral (N) lines. The filter is composed of a common-mode choke and three capacitors. L_1 and M are respectively the inductance of one winding and the mutual inductance between windings. By convention, two types of capacitor are distinguished in this type of filter:

- An X capacitor (C_X) is placed between L and N lines
- Y capacitors (C_Y) are placed between L or N to the earth (E)

L

L_1

L

Interference
source

C_X

M

Load

N

L_1

N

C_Y C_Y

E

E
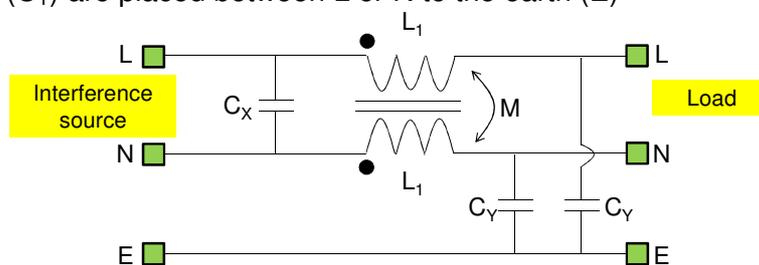
1. What kind of filter is this (low-pass, high-pass or pass-band)?

2. In the event of common-mode disturbance (the common-mode current circulates on L and N lines in the same direction), which filter components attenuate the common-mode noise?

3. Same question for a differential-mode disturbance (the differential-mode current flows along the L line and returns through the N line).

4. Why is it better to use a common-mode choke instead of two uncoupled inductors?

5. We use the following values for the passive devices: C_X = 100 nF, C_Y = 1 nF, L_1 = 1.1 mH. Mutual coupling coefficient K between the choke windings is equal to 0.9977. We assume that the filter devices are ideal (no stray components). We also assume that the noise source and load impedances are equal to 50 Ω. The influence of L and N lines and earth chassis will be neglected.

With IC-EMC, build a schematic diagram to compute the filter's attenuations of CM and DM noise between 10 kHz and 100 MHz. Express them in terms of insertion loss IL (dB). Remember that IL is the ratio of the load voltage without the filter, divided by the load voltage when the filter is connected between the disturbance source and the load.

6. We now consider realistic models of passive devices. The common-mode choke model presented in Fig. 5-31 (Würth Elektronik 744824101) is considered. The models Murata GA255DR7E2104 and GA242QR7E2102 are used for C_X and C_Y capacitors respectively. From the impedance measurements of both capacitors (book/ch5/Cx_Murata_Z.s1p and book/ch5/Cy_Murata_Z.s1p), build their electrical models.

7. Repeat question 5 with realistic models of the passive devices. Compare the insertion losses with those computed in question 5. Draw conclusions about the influence of the stray components of passive devices on EMI filter characteristics.

8. What constraints must be taken into account when selecting the common-mode choke and the C_X and C_Y capacitors?

Corrections:

1. EMC filters always stands for low-pass filtering. In the AC line, the EMI filter purpose is to attenuate high-frequency components of an electromagnetic disturbance conducted along the power line and prevent from unwanted radiation. A rapid analysis of the filter confirms this statement (see answers to questions 2 and 3).

2. The figure below presents the equivalent circuit of the filter in case of common-mode (CM) disturbance. The circulation of the CM current is pointed out. Clearly, the X capacitor has no influence on the CM current since no CM current flows through C_X. As CM current flows in the same direction through both winding of the common-mode choke, the magnetic flux is accumulated in the magnetic core resulting in a large CM inductance L_{CM} equal to $L_{CM} = \dfrac{L_1}{2} + \dfrac{M}{2}$. This impedance which becomes larger at higher frequency blocks the CM current. Moreover, the CM current is bypassed by Y capacitors at high frequency beforfe reaching the load.

The CM choke and the Y capacitors are reponsible of the suppression of CM noise.
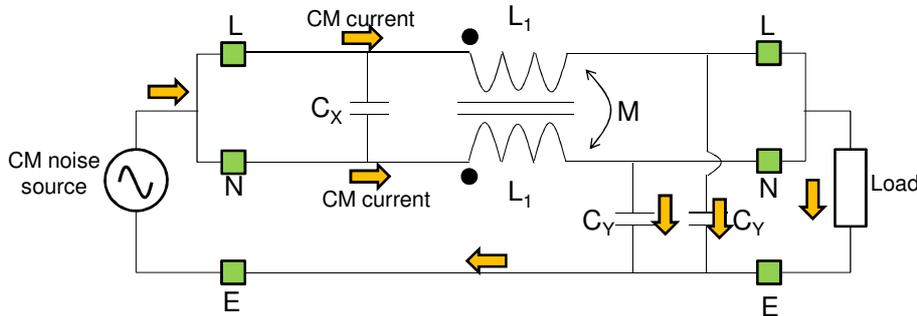
3. The figure below presents the equivalent circuit of the filter in case of differential-mode (DM) disturbance. The circulation of the DM current is pointed out. The C_X capacitor bypasses the DM current from the L line to the N line.The C_Y capacitors contribute also to bypass the DM current, but to a smallest extent than C_X capacitor.

As DM current flows in opposite directions through both winding of the common-mode choke, the magnetic flux should be cancelled if the CM choke was perfect (no leakage inductance). In a real CM choke, the leakage or differential-mode inductance is not null but far smaller than the CM inductance.The DM inductance L_{DM} is equal to $L_{CM} = 2L_1 - 2M$. The DM inductance contributes also to block the DM current.

The CM choke and the X capacitors are the main devices reponsible of the suppression of DM noise.
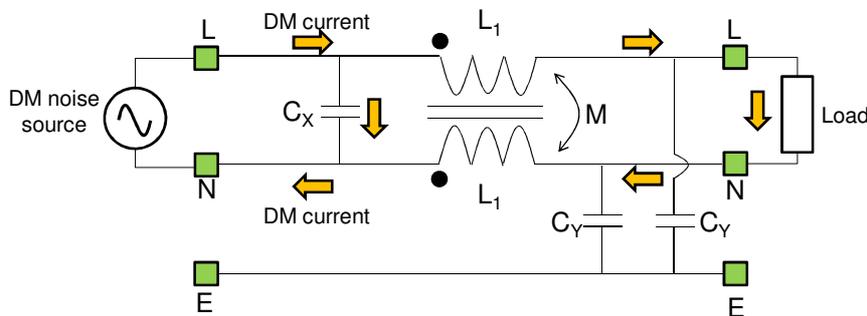
4. The two figures below show the equivalent circuit of the filter in case of CM and DM disturbances, when two uncoupled inductors are mounted on L and N lines.Uncoupled means that there is no magnetic coupling between inductors → M = 0. We suppose that both inductors are identical with a self-inductance L_1. In the case of a CM disturbance, the CM current circulates in the same direction through both inductors resulting in a common-mode inductance equal to $L_1/2$, which is nearly half the CM inductance of the CM choke. Thus, the CM suppression would be less efficient with two uncoupled inductors compared to the solution with a CM choke.

However, as the inductors are uncoupled, the DM inductance is equal to $2\times L_1$, which is far larger than the DM inductance with the solution with the CM choke. The DM noise suppression would be more efficient. Contrary to CM signals, we do not want to eliminate all DM signals ! Indeed, the AC power transfer between the source and the load is done according to a DM. As the AC current is large, the magnetic flux generated in both inductors L_1 could be large enough to make saturate the magnetic core, resulting in distorsions of the AC current. In contrast, as the magnetic flux induced

by DM current in the magnetic core of the CM choke nearly cancels, the AC current would not make the magnetic core saturate.

For AC 220 V line, the power quality is measured according to the 50 Hz harmonic distorsion.
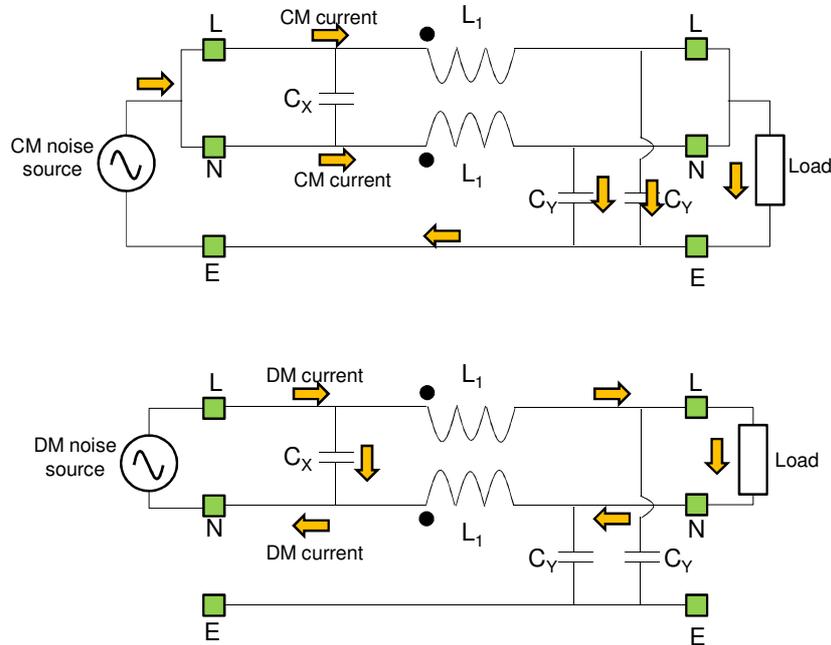
More generally, for differential lines (power or signal transmission), CM noise is usually more problematic and thus it has to be suppressed. It is better to use CM choke, which filters efficiently the CM noise without affecting the wanted DM signals.

5. The following figure presents the schematic used to simulate the insertion loss of the EMI filter in case of DM disturbance (the earth is not represented since no DM current circulates on it).The schematic name is IL_DM_noise_ideal.sch. Vemi and Remi are the DM noise source and equivalent output impedance. Differential voltage probes are placed across the loads. AC simulation is configured to plot the evolution of the voltages induced across the load vs. frequency.
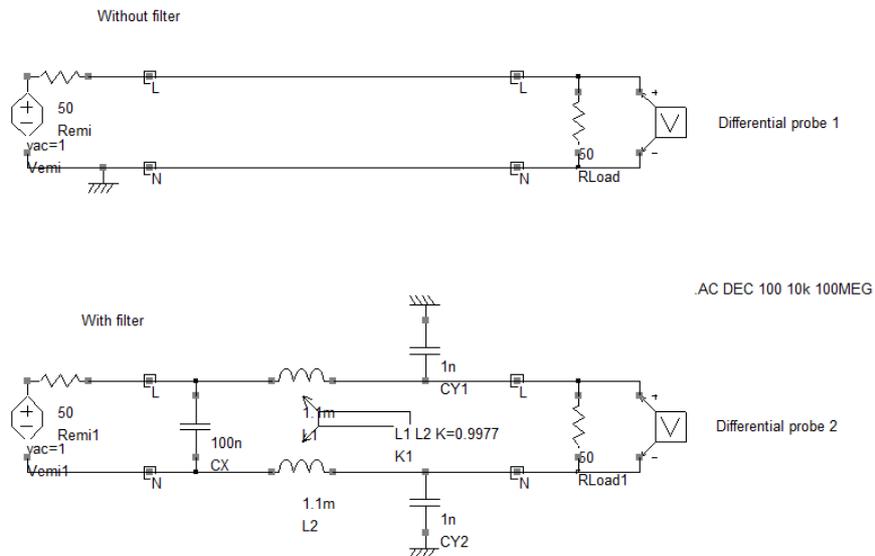
The following picture presents the simulation results of the differential voltages across the load, without and with the filter, expressed in dB. The IL is the differences between both curves. The results shows that the cutt-off frequency of the filter to DM noise is about 65 kHz. The filter roll-off is 20 dB/dec up to 2 MHz and then 60 dB/dec.

The following figure presents the schematic used to simulate the insertion loss of the EMI filter in case of CM disturbance.The schematic name is IL_CM_noise_ideal.sch. Vemi and Remi are the DM noise source and equivalent output impedance. Common-mode voltage probes are placed accross the loads.

The following picture presents the simulation results of the CM voltages across the load, without and with the filter, expressed in dB. The IL is the differences between both curves. The results shows that the cutt-off frequency of the filter to CM noise is about 15 kHz. The filter roll-off is 20 dB/dec up to 2 MHz and then 40 dB/dec.
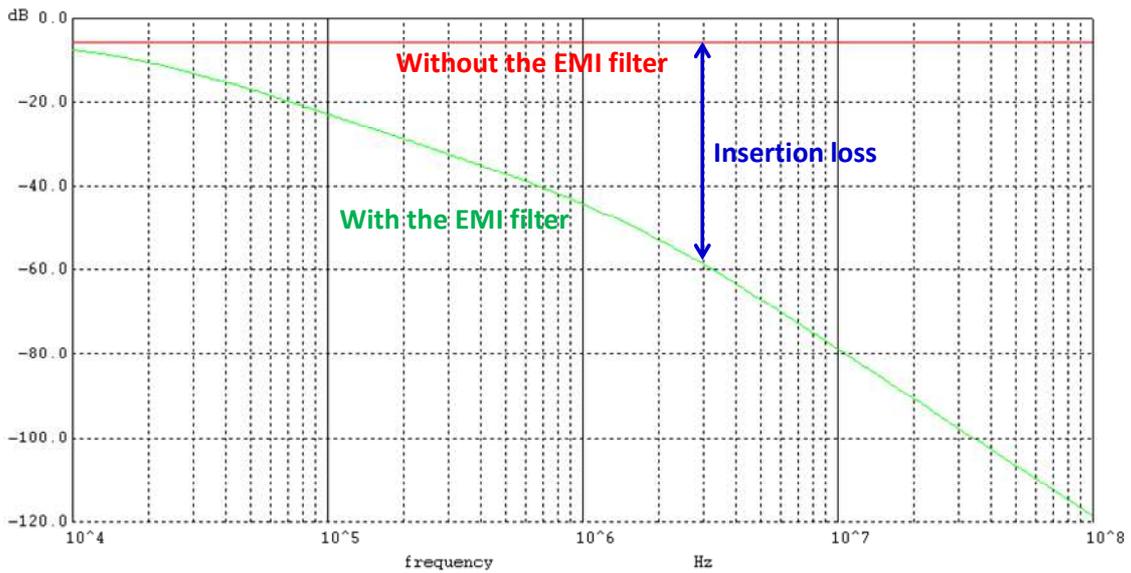
6. Simplified version of the model of GA255DR7E2104 (Cx_Model_Murata.sch) and comparison between measured and simulated impedance (EMC / S parameters ⊛):
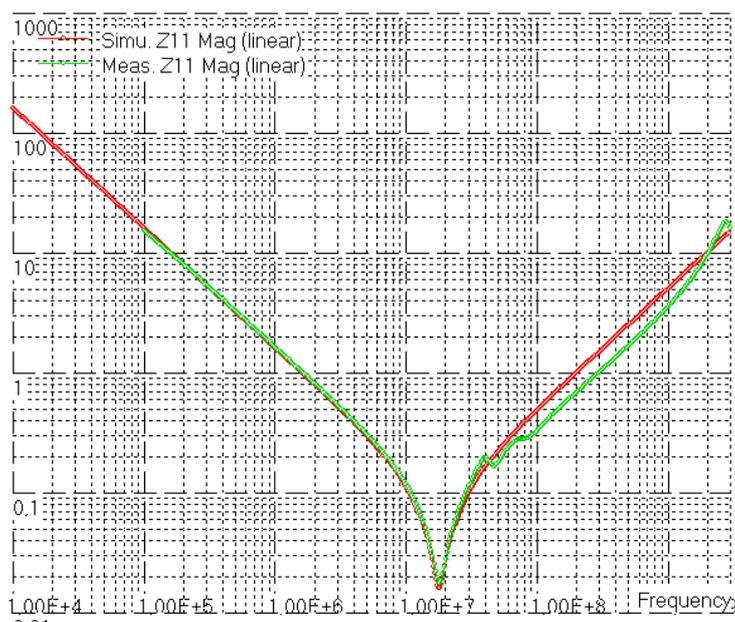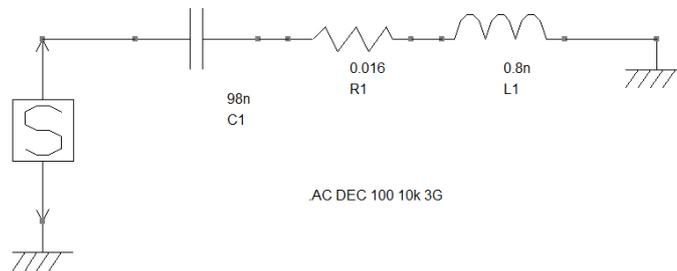
Simplified version of the model of GA242QR7E2102 (Cy_Model_Murata.sch) and comparison between measured and simulated impedance:
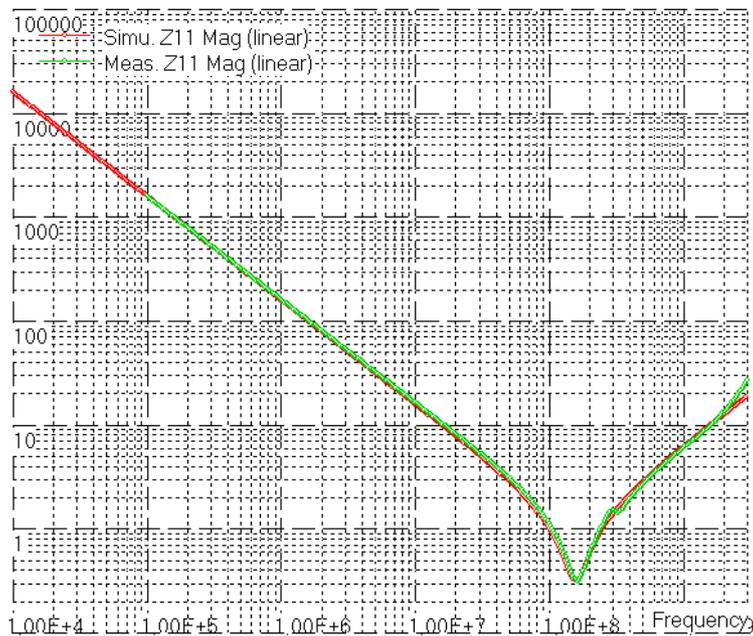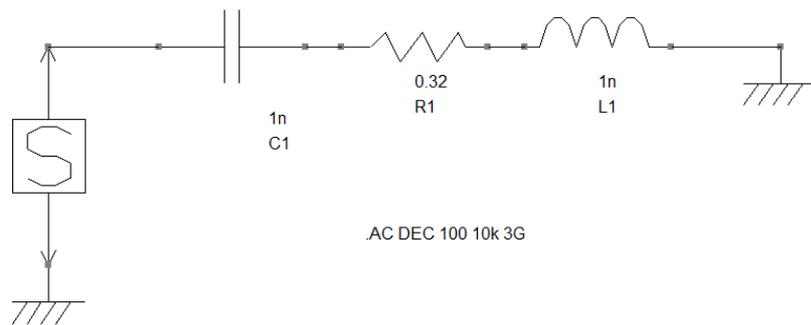
7. Circuit model for the computation of insertion loss of the filter in case of DM disturbance (IL_DM_noise_real.sch).Comparison with the results of question 5 shows that the IL is similar to the ideal model version up to 10 MHz, because the capacitor Cx cannot be considered as a pure capacitance above this frequency (see previous question). Moreover, the DM inductance of the CM choke is no more a pure inductance above 15 MHz (see Fig. 5-32). Above 20 MHz, the IL stops increasing.The IL does not exceed 100 dB ,which is a very high value.
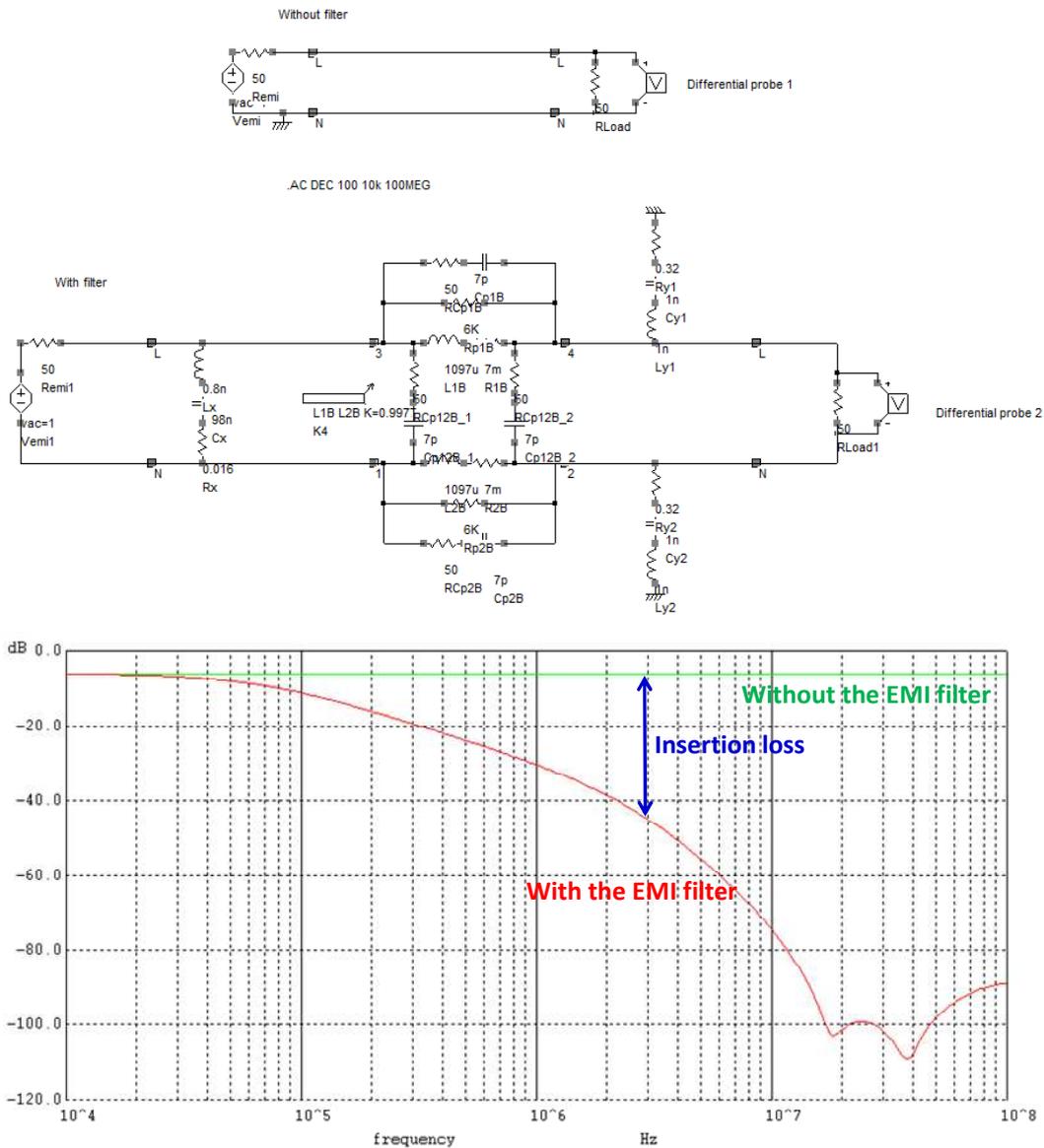
Circuit model for the computation of insertion loss of the filter in case of CM disturbance (IL_CM_noise_real.sch).Comparison with the results of question 5 shows that the IL is similar to the ideal model version up to 350 kHz. Above this frequency, the CM inductance of the choke is no more a pure inductance. As shown in Fig. 5-32, a lossy behaviour appears and the self- resonance arises at nearly 1 MHz. Due to the stray components of the passive devices, the IL does not exceed 50 dB.
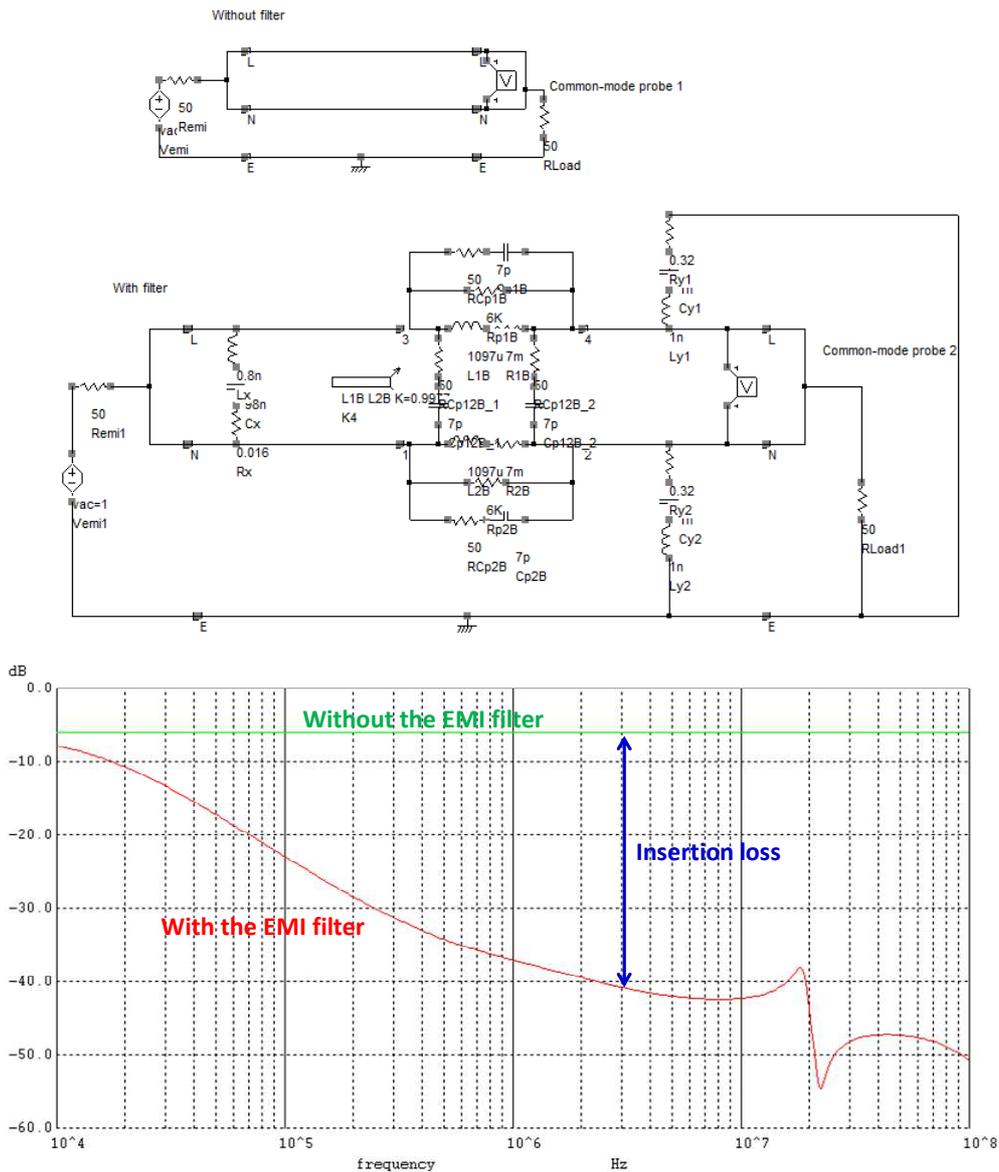
The stray components have to be taken into account to estimate realistic performances of the EMI filter, especially for the CM disturbance suppression.

8. The choice of the passive devices forming the EMI filter depends on several criteria. For the CM choke, the max. current and the saturation current have to be considered to ensure that the magnetic core will not saturate due to the AC current. Other constraint such as the temperature range and the temperature stability may be taken into account.

For C_X and C_Y capacitors, the maximum voltage have to be sufficient (e.g. a minimum of 250 Vac is required for AC lines). The robustness to high voltage pulse, transient, or bursts have to be verified, since such disturbances are commonly observed on AC power supply lines. Operating temperature range and temperature stability may also be taken into account.

EXERCISE NO 3 - THREE-TERMINAL CAPACITOR

The purpose of this exercise is to compare the filtering performance of two different types of ceramic 100 nF capacitor:

- a two-terminal version: X7R, reference Murata GCM21BR71H104KA37L
- a three-terminal version: Murata NFM21PC104R1E3

Both are mounted in a 0805 case (imperial code). The following diagram compares the principles of a traditional (two-terminal) and a three-terminal capacitor mounted as a bypass element to filter conducted noise. The external structure of the devices is also described.

Both devices have been characterised with a VNA. The measurement files are book/ch5/Capa_ceramic_100n.s2p for the two-terminal version, and book/ch5/NFM21PC104R1E3.s2p for the three-terminal version.
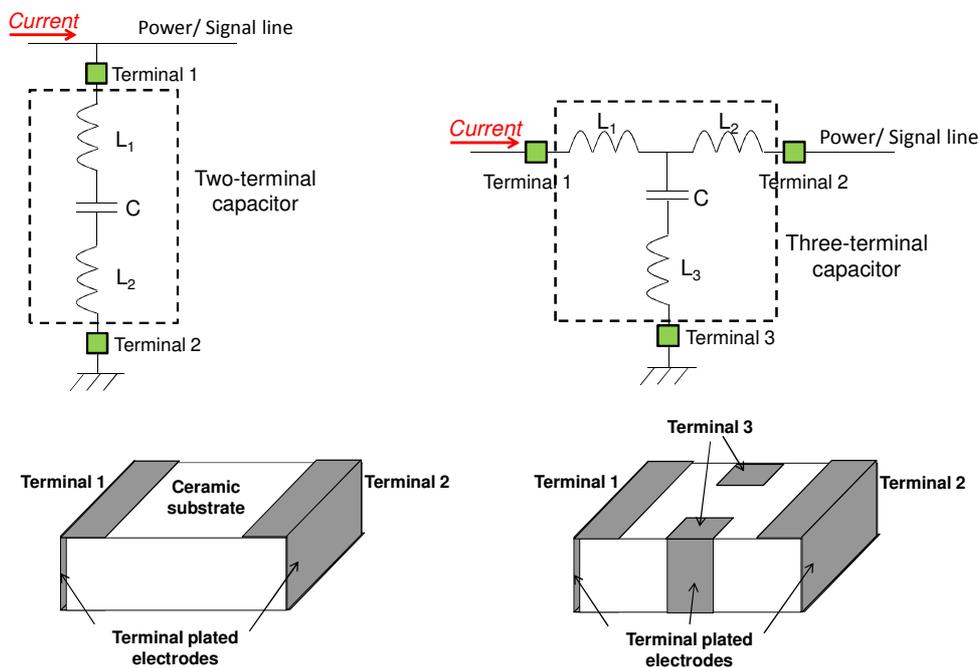
1. Initially, we assume that lead inductances are identical in two- and three-terminal capacitors and equal to L. What is the ratio between the equivalent series inductance (ESL) of two- and three-terminal capacitors?

2. Why does a low ESL constitute an advantage for an EMI filter? Do the L1 and L2 inductances degrade the filtering performance of the three-terminal capacitor? Do they degrade the filtering performance of the two-terminal capacitor?

3. What are the dimensions of the capacitor package in millimetres?

4. Why is the third terminal of the Murata NFM21PC104R1E3 placed on both sides of the device?

5. Using the S-parameter measurements of the capacitors, propose equivalent electrical models for both capacitors in the 100 kHz to 3 GHz range.

6. Compare the ESL and self-resonant frequencies of both capacitors.

7. Both capacitors are used to filter a single-ended line excited by a noise source with a series impedance equal to 50 Ω and terminated by a constant impedance of 50 Ω. With IC-EMC, propose a schematic diagram to compute the attenuation offered by both capacitors. Compare their attenuation and draw conclusions about the advantage(s) of the three-terminal capacitor.

Corrections

1. The ESL is the parasitic inductance placed in serie with a capacitance, i.e the inductance crossed by current that flows through the capacitance and the ground refererence. For the two-terminal capacitor, the ESL is equal to 2xL, while the ESL is only equal to L for the three-terminal capacitor. If the terminals have the same parasitic inductance, the ESL of the three-terminal capacitors is twice smaller than the ESL of the two-terminal capacitor.

2. A parallel capacitor forms a good EMI filter since it bypasses the high frequency noise. But the ESL limits the frequency range of a filtering capacitor since it increases the impedance of the capacitor above the self-resonant frequency. Reducing the ESL increases the frequency range of a capacitor for an EMI filter. Inductances L1 and L2 contribute to the ESL of the two-terminal capacitor and thus reduce its frequency range.

Two terminals of the three-terminal capacitor introduce inductances L1 and L2 in series to the signal path. They do not contribute to the ESL of the capacitor but they constitute a blocking elements for high frequency noise circulating on the signal path. Actually, the three-terminal capacitor constitutes a T-type filter, as shown in exercise 3 of chapter IV.

3. 0805 is a code for passive device case dimensions. According to Table 5-1, the dimensions WxLxH are equal to 0.08 in × 0.05 in × 0.018 in, i.e. 2.0 mm × 1.2 mm × 0.45 mm.

4. The ESL of the three-terminal capacitor is mainly due to the ground terminal, i.e. terminal 3. Minimizing L3 reduces the ESL and improves the filtering performances. Duplicating the third terminal on both sides of the device nearly divides by 2 the inductance L_3. Moreover, it ensures a symmetrical PCB design, which is always better to reduce common-mode.

5. The model of the two-terminal capacitor (Murata GCM21BR71H104KA37L) has already been constructed in part 5.3 (see Fig. 5-15).

A simple model version of the three-terminal capacitor is proposed below (model_simple_NFM21PC104R1E3.sch). Click on ▶ to generate the SPICE netlist and launch the simulation. At the end the simulation, open the S parameter interface ⊛. Import the measurement file NFM21PC104R1E3.s2p to compare measured and simulated S11 and S12 parameters.

Measurement and simulation results do not fit perfectly, especially near the self-resonant frequency. The model overestimates the self-resonant frequency (97 MHz in simulation, 57 MHz in measurement). However, the model describes the evolution of the impedance correctly and shows the difference of inductance measured from Z11 and Z12 measurements.
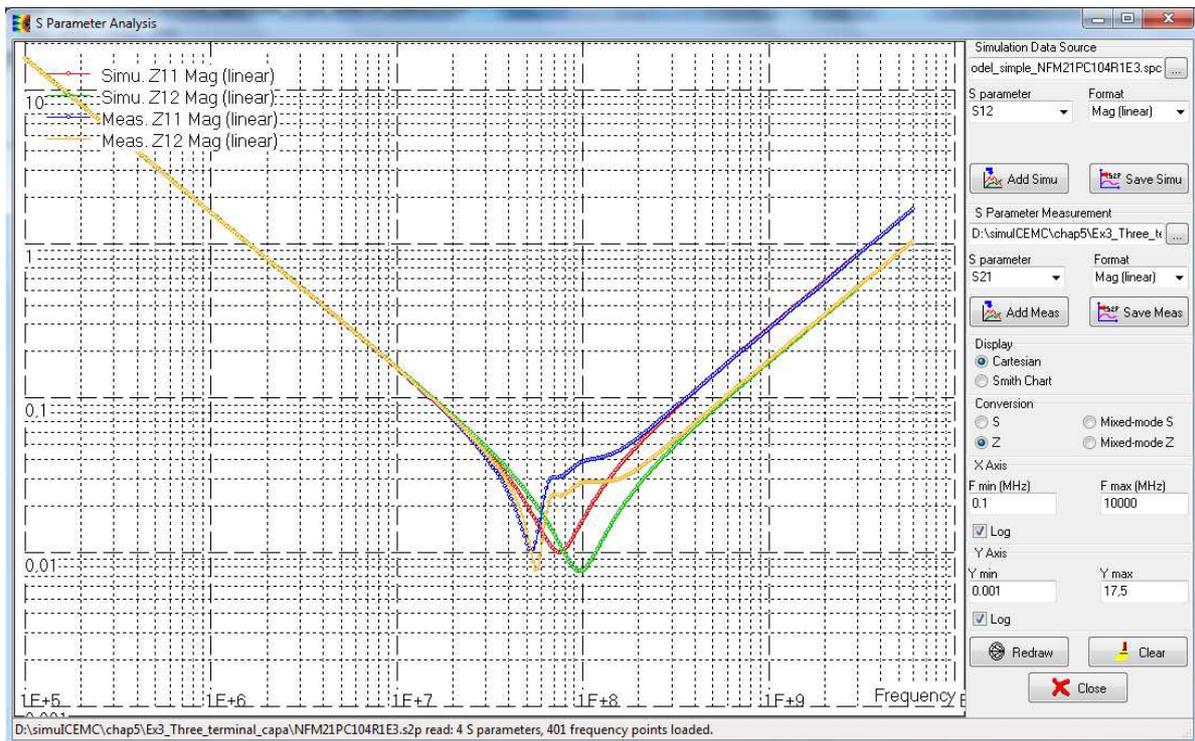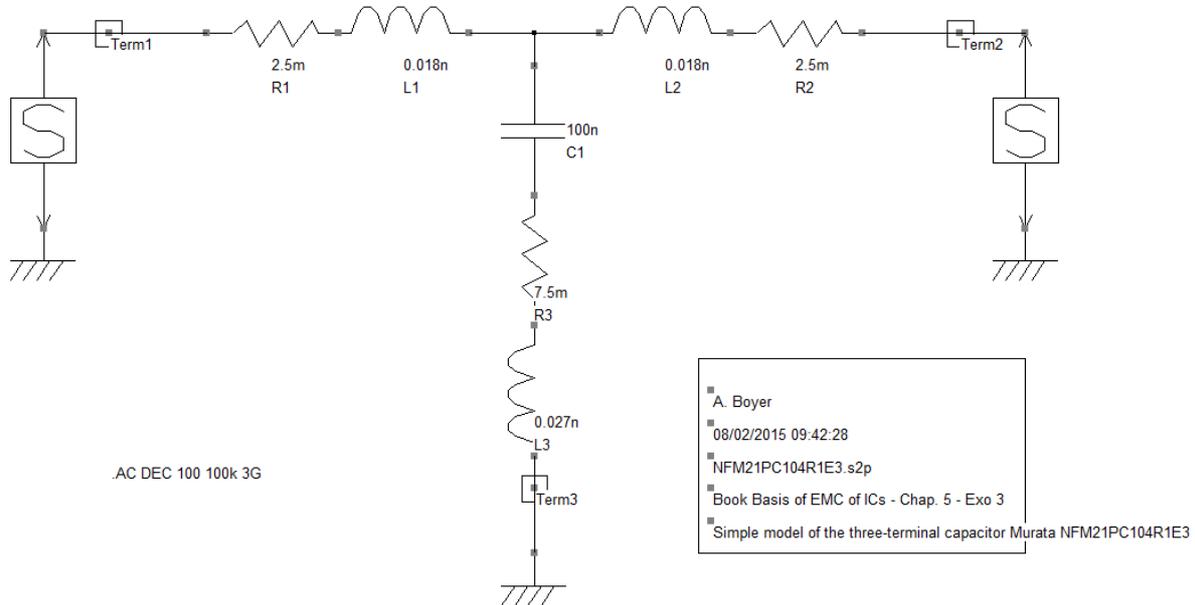
6. The ESL of the two-terminal capacitor is 0.7 nH and the self-resonant frequency is 19 MHz.

Based on the simple model version, the ESL of the three-terminal capacitor is 0.027 nH and the self-resonant frequency is 96 MHz. Even if both devices are mounted in package with the same dimensions, the ESL is considerably lowered with the three-terminal construction.

7. The following picture presents a model for the simulation of the attenuation provided by both capacitors, with source and load impedances equal to 50 Ω. Here, the simple model version of the three-terminal capacitor is used. The model neglects the influence of the signal traces between the noise source and the load. The schematic diagram is given in the file comparison_IL_capacitors.sch.

Two voltage probes configured in dB display are placed across the terminal loads. The noise source generator is a 1 V sinus waveform. A small signal analysis from 100 kHz to 3 GHz is set.
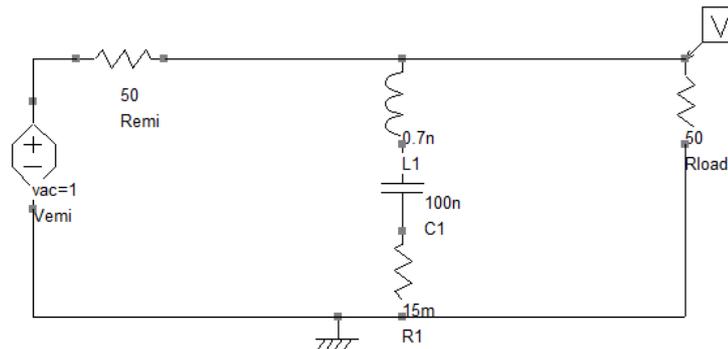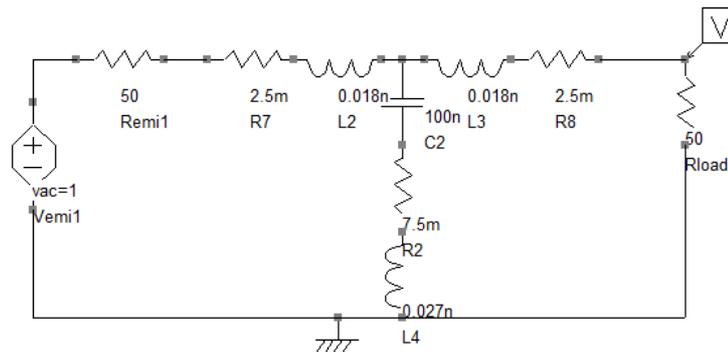
The following graph compares the attenuation provided by both capacitors. The filtering performances are identical up to 10 MHz. The self-resonant frequency of the three-terminal capacitor is 6 times larger than the two-terminal capacitor. Above the self-resonant frequency of the three-terminal capacitor, its attenuation is 30 dB better than that of the two-terminal capacitor, due to the small ESL. Clearly, using a three terminal capacitor provides better filtering performances in the 10 MHz - 3 GHz range.

The effect of trace routing and connection of the capacitors have not been taken into account in the model. These parameters have an influence and may degrade the attenuation in high frequency.To obtain such good results, the placement and routing of the three-terminal capacitor have to be careful: the connection of terminal 3 to the ground must be done with short and wie trace to reduce its parasitic inductance.